Hindawi Publishing Corporation
Shock and Vibration
Volume 2015, Article ID 817598, 19 pages
http://dx.doi.org/10.1155/2015/817598

Research Article

Experimental Investigation of Ultrasonic Vibration Assisted Turning of 304 Austenitic Stainless Steel

Ping Zou,[1] Yingshuai Xu,[1] Yu He,[1,2] Mingfang Chen,[1] and Hao Wu[1]

[1]*School of Mechanical Engineering and Automation, Northeastern University, Shenyang 110819, China*
[2]*Department of Mechanical Engineering, Northwestern University, Evanston, IL 60208, USA*

Correspondence should be addressed to Yingshuai Xu; xuyingshuai@126.com

Received 10 May 2015; Revised 4 August 2015; Accepted 4 August 2015

Academic Editor: Jörg Wallaschek

This research study focuses on the experimental analysis of the three-dimensional (3D) surface topography and surface roughness of the workpiece machined with ultrasonic vibration assisted turning (UAT) in comparison to conventional turning (CT). For the challenge that machining difficulties of 304 austenitic stainless steel (ASS 304) and high demands for the machined surface quality and machining precision represent, starting with cutting principle and processing technology, the ultrasonic vibration method is employed to scheme out a machining system of ultrasonic vibration assisted turning (MS-UAT). The experiments for turning the workpiece of ASS 304 are conducted with and without ultrasonic vibration using the designed MS-UAT, and then the 3D morphology evaluation parameters *Sa* and *Sq* are applied to characterize and analyse the machined surface. The experimental results obtained demonstrate that the process parameters in UAT of ASS 304 have obvious effect on the 3D surface topography and surface roughness of machined workpiece, and the appropriate choice of various process parameters, including ultrasonic amplitude, feed rate, depth of cut, and cutting speed, can enhance the machined surface quality efficiently to make the machining effect of UAT much better than that of CT.

1. Introduction

In recent decades, there is an increasing demand for the surface quality and machining precision of highly sophisticated products and precision components on the machinery industry [1]. At the same time, novel materials appear continuously, and various difficult-to-cut materials have gained widespread application in the mechanical manufacturing [2]. Furthermore, the shape of workpiece becomes increasingly complicated, and the requirement of surface roughness and precision and some special requirements also become higher and higher [3]. In view of the above, higher requirements are raised for the machining technology, since the conventional machining technology has been difficult to meet the requirements of the processing [2–5].

Considering the productivity, metal removal amount, and machining quality, turning process is still an extensively used method of machining [6–8], as well as an economic and practical way of machining. For CT technique, as it is usually accompanied by the problems containing big cutting force, high cutting temperature, and chip removal difficulties in cutting process, these can lead to serious cutting tool wear and short lifetime, and so forth; thus the processing efficiency is reduced and the cost of machining is increased. Due to the existence of significant limitations, CT is hard to satisfy the processing requirement. UAT has been proposed in such conditions, and the research on UAT has been carried out.

Ultrasonic vibration assisted machining is a compound machining method, combining ultrasonic vibration with ordinary cutting, and has high application value in machining difficult-to-cut materials [9, 10]. UAT is a method with a periodic vibration added to the CT to change continuous cutting mechanism of CT approach. In UAT, cutting tool and workpiece are periodically separated and contacted, which makes the size and direction of cutting speed periodically changed and also makes the UAT of difficult-to-cut materials or difficult-to-cut processes much more effective, which is difficult to achieve by CT, leading to the reduction of cutting

force [11, 12] and the decrease of cutting temperature [13, 14], and so forth. All of the excellent effects of UAT process have got extensive attention [11–16].

Babitsky et al. [13, 17] adopted UAT method to machine the aviation materials. It was demonstrated that the UAT method performed better at lower cutting speed with high frequency and high amplitude of vibration. Having studied the effect of machining parameters during UAT of Inconel 718, Nath and Rahman [18] found that the ultrasonic vibration cutting mechanism was influenced by three important parameters: tool vibration frequency, tool vibration amplitude, and workpiece cutting speed that determine the cutting force. Patil et al. [14] studied the effect of ultrasonic vibrations on machining of Ti6Al4V. The study showed that the surface roughness in UAT was lower than that in CT, and the UATed surfaces had matte finish against the glossy finish on the CTed surfaces. Maurotto et al. [11] developed and tested an improved UAT setup for machining of a β-titanium alloy, which resulted in substantial reductions in the cutting forces and was achieved with a concomitant improvement in the surface quality of machined specimens, compared to CT with the same cutting parameters.

The austenitic stainless steel has enjoyed wide use in industry for its excellent mechanical properties; however, it is also known as a typical difficult-to-cut material for the low thermal conductivity, active reactivity, and short interface between the tool and the chips, high cutting temperature, small modulus of elasticity, and so forth. Vivekananda et al. [2, 19] designed and analysed an ultrasonic vibratory tool using finite element method, studied the difference between UAT and CT of stainless steel, and found that the UAT could reduce the cutting forces as well as surface roughness comparing with CT and was very suitable for machining hard material like stainless steel whereas Vivekananda et al. did not make the experimental investigation and analysis in detail. And a few of the documents are about the UAT of austenitic stainless steel in the preexisting documents. The difficulty of austenitic stainless steel processing could be solved by the designed MS-UAT in the paper.

Ultrasonic vibration system is of significant importance in the ultrasonic vibration assisted machining [20, 21]. Whether the design of ultrasonic vibration system is reasonable or not has direct effect on the practical application of UAT, so it is crucial and urgent to study the theory of design and analytical method of ultrasonic vibration system. In order to study UAT further, it is necessary to study the MS-UAT deeply to ensure high machining precision and quality. Thus the developed MS-UAT will improve and enhance the stability of processing device, the effect of chip breaking and removing, the machining quality, the lifetime of cutting tool, and so forth.

The machined surface quality of workpiece not only affects work precision, connection strength, smoothness of movement, leakproofness, abrasion resistance, and useful life of various mechanical products, but also is related to noise magnitude of machine which is working on it. Therefore, it is vitally important to study and solve the problems of surface topography and surface roughness of workpiece. Reasonably evaluating machined surface quality has practical significance for mass production and economic efficiency. Along with the development of all kinds of testing technology and digital processing technology, the 3D characterization technique of machined surface has already been developed and has shown a tremendous advantage. This study is intended to make use of 3D morphology evaluation parameters to characterize and analyse the machined surface.

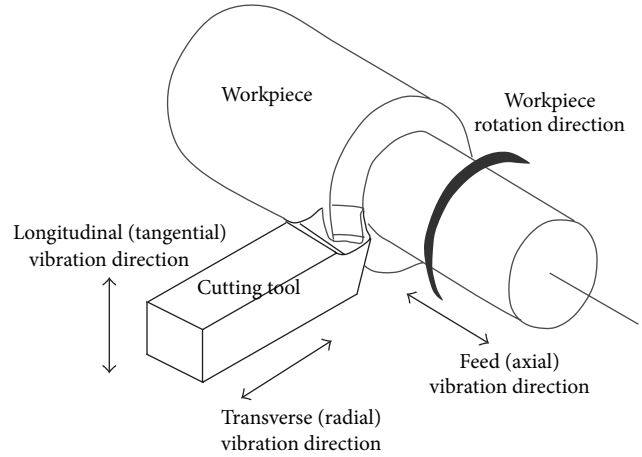

Figure 1: Principal vibration directions in UAT.

This paper designs the ultrasonic vibration system and special fixture, which are used on the CA6140 type lathe, and sets up the MS-UAT. The finite element method is used to determine the parameters of ultrasonic horn, namely, its length and cross-sectional area and so forth, when the resonance frequency is 20 kHz. Afterwards, the design of ultrasonic horn is optimized. Under the same condition, the established MS-UAT is applied to make UAT and CT experiments, respectively, and contrastively analyse the 3D surface topography and surface roughness of machined workpiece. Additionally, the influence of ultrasonic amplitude, feed rate, depth of cut, and cutting speed on machined surface quality in the UAT of ASS 304 with cemented carbide coated cutting tool is studied and analysed. To ensure high machining precision and quality is the essential requirements of UAT in the production development and science experiment. The investigation will provide theoretical and practical data for the UAT technique of ASS 304 as well as promoting the further development and application of UAT.

2. Design of MS-UAT

UAT can generally be categorized by vibration direction as follows: feed (axial) vibration turning, longitudinal (tangential) vibration turning, transverse (radial) vibration turning, and complex vibration (2D) turning. Figure 1 shows the principal vibration directions in UAT [17, 22].

Longitudinal (tangential) vibration turning was chosen, and light weight cutting tool (cemented carbide cutting tool) was selected in this study; thus, it was unnecessary to measure and ascertain displacement and node of the ultrasonic cutting tool so that it could be used expediently. In the meantime, height adjusting mechanism of the tool nose was designed

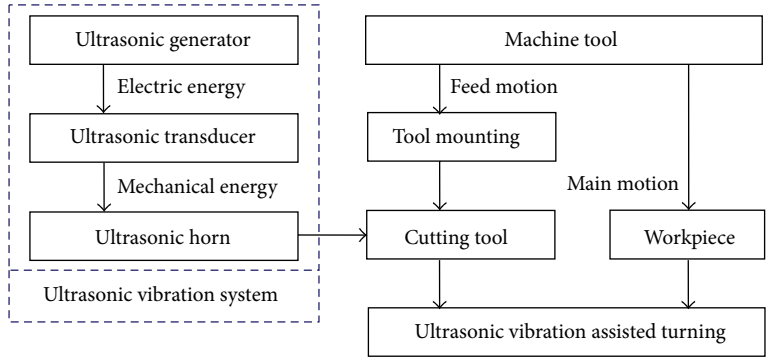

Figure 2: Structure and working principle diagram of MS-UAT.

simply, the cutting tool was prone to be disassembled, and resonance state was easy to be set. Additionally, the system of longitudinal vibration was characterized by big vibrational power transmitting and low vibrational energy loss. But this device needed to adopt the rigid fastening ultrasonic horn and the ultrasonic horn should have considerable stiffness.

MS-UAT mainly consists of two large divisions, namely, machine tool and the device of ultrasonic vibration. The device of ultrasonic vibration contains ultrasonic vibration system, cutting tool, and other necessary components. The device of ultrasonic vibration enables the cutting tool to obtain a certain amplitude for ultrasonic vibration and fix the ultrasonic vibration system and cutting tool onto the tool mounting to make UAT come true. Figure 2 shows the structure and working principle diagram of MS-UAT.

A method, by which the CA6140 type general-purpose lathe was converted into the lathe of UAT through installing the device of ultrasonic vibration on the general-purpose lathe, was carried out in the study. The establishment of MS-UAT could be refined into the work of the following parts: the design of ultrasonic vibration system, the fixture (i.e., tool mounting) design of ultrasonic vibration system, the integral installation of MS-UAT, and so forth.

2.1. Design of Ultrasonic Vibration System. The ultrasonic vibration system converts 220/380 V alternating current into ultrasonic-frequency electric oscillation signals with the power and frequency, respectively, as 300 W and over 16 kHz through ultrasonic generator and then adds electrical signals to ultrasonic transducer to make it generate mechanical vibrations with the same frequency, and this vibration is amplified by ultrasonic horn [23]. Ultimately, considerable amplitude of mechanical vibration is generated on the end of the cutting tool. The ultrasonic vibration system is principally composed of ultrasonic generator, ultrasonic transducer, and ultrasonic horn as shown in Figure 3.

As the technique of the ultrasonic generator and ultrasonic transducer has been relatively mature, they can be directly chosen. In this study, in the light of the design requirements, 2000bdc type ultrasonic generator and ultrasonic transducer manufactured by American BRANSON Ultrasonics Corporation were employed. The essential parameters of the 2000bdc type ultrasonic generator were the

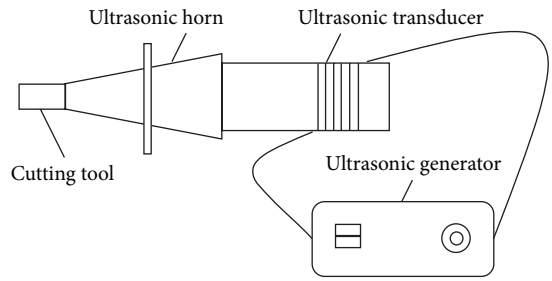

Figure 3: Structure sketch of ultrasonic vibration system.

alternating current power with operating voltage of 200~240 V, frequency of 50 Hz, output power of 1100 W, and output frequency of 20 kHz. The selected ultrasonic transducer was a piezoelectric transducer with small volume, high electroacoustic conversion efficiency, and small calorific value. A signal with specific frequency was generated by the ultrasonic generator, and it could be a sine signal or a pulse signal. The specific frequency referred to the frequency of ultrasonic transducer. The frequency signal generated by ultrasonic generator went through a power amplifier and then went through impedance matching to enable the output impedance to be consistent with the ultrasonic transducer, thus driving ultrasonic transducer to convert the electric signals into the mechanical vibrations.

One of the major functions of the ultrasonic horn in the ultrasonic vibration system is to amplify the particle displacement or velocity of mechanical vibration and focus the ultrasonic energy on a small area. In UAT, the amplitude of cutting tool generally needs dozens to hundreds of micrometers, but the output amplitude of piezoelectric ultrasonic transducer is habitually only 4~10 μm. Hence, it is necessary to connect the transducer with ultrasonic horn to amplify the amplitude of mechanical vibration. Finally, the ultrasonic vibration with larger amplitude is transferred to the cutting tool and then realizes the UAT of workpiece. Due to the differences of MS-UAT, the ultrasonic horn needs custom design in accordance with the actual machining requirements and the existing equipment conditions.

The design of ultrasonic horn was considered by the half-wave and no-load, and then it was adjusted appropriately

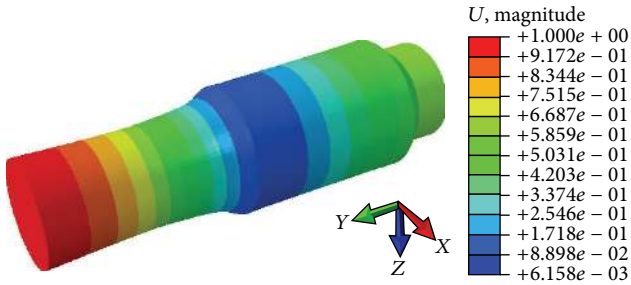

Modal analysis of ultrasonic horn
ODB: horn.odb Abaqus/standard 6.14-1 Wed May 06, 00:24:21
Central daylight time 2015
Step: modal analysis
Mode 10: value = 1.58974E + 10 freq. = 20067 (cycles/time)
Primary var.: U, magnitude
Deformed var.: U deformation scale factor: +1.390e + 01

Figure 4: Modal analysis chart of ultrasonic horn.

in the actual application. The ultrasonic horn used in UAT was an upper-thicker and down-thinner metal rod, and the large end of ultrasonic horn was connected with the ultrasonic transducer and the small end of ultrasonic horn was connected with the tool holder. The modal analysis of the designed ultrasonic horn was carried on through ABAQUS simulation software. The modal analysis chart is shown in Figure 4.

The process of all the design calculation of the ultrasonic horn was based on the theory of stepped ultrasonic horn of half-wavelength and circular section. The stepped ultrasonic horn had great stress concentration when the cross section was abruptly changed. And close to the small end of the stepped ultrasonic horn, it was easy for the pole to form fracture caused by fatigue occurring; thus here, the place of the abrupt change was made into changeover portion of specific modality. In addition, for the sake of decreasing the energy loss, a cylindrical section with the same diameter of the ultrasonic transducer was added onto the input end of the ultrasonic horn and transited to large end of the stepped ultrasonic horn through changeover portion.

The resonance frequency is defined as 20 kHz, and 45 steel (density $\rho = 7890\ \text{kg/m}^3$, elastic modulus $E = 209$ GPa, and Poisson's ratio $\sigma = 0.269$) is selected as the material of ultrasonic horn. The dimension and property of the ultrasonic horn can be determined by the following equations:

$$\begin{aligned} N &= \frac{D_1}{D_2} = 1.34, \\ \lambda &= \frac{C}{f} = 258\ \text{mm}, \\ x &= \frac{\lambda}{4} = 64.5\ \text{mm}, \\ a &= b = x = 64.5\ \text{mm}, \\ l &= a + b + l_0 = 142\ \text{mm}, \end{aligned} \tag{1}$$

where $D_1 = 51$ mm and $D_2 = 38$ mm are the ultrasonic horn diameter in large end and small end, respectively; $C = 5169$ m/s is the longitudinal vibration velocity in ultrasonic horn material; $l_0 = 13$ mm is the cylindrical section length of ultrasonic horn; a and b are the length of ultrasonic horn in large end and small end, respectively; N, λ, f, x, and l are the area factor, wave length, resonance frequency, displacement node length, and the theoretical resonance length of ultrasonic horn, respectively.

The physical length of the ultrasonic horn designed by finite element method was 139 mm after optimizing processing. As shown in Figure 4, the resonance frequency of the ultrasonic horn was 20.067 kHz, which approximated to theoretical design requirements.

2.2. Fixture Design of Ultrasonic Vibration System and Integral Installation of MS-UAT. To establish MS-UAT on the machine tool it is needed to design the special fixture for installing the ultrasonic vibration system. There was a strict requirement for the height of the tool nose of cutting tool during designing. And the tool nose had better have an amplitude value lower than the center of workpiece rotation. When the cutting tool vibrated, the tool nose was exactly in the center of workpiece rotation. Providing that the tool nose was higher than the center, the cutting tool could not deviate from the workpiece when the vibration was removed, and there was a high friction between the flank face of the cutting tool and the workpiece. It could lead to several phenomena that the cutting force was increased and the low-frequency oscillation mark, well-regulated and shiny, was besprinkled in the machined surface. Providing that the tool nose was much lower than the center of workpiece rotation, the tool nose was not in the center of workpiece rotation when the cutting tool vibrated. It would give rise to several phenomena that the road of tool nose was increased and the low-frequency oscillation mark, which was white but not shiny, was besprinkled in the machined surface. Of course, it was extremely hard for the tool nose of cutting tool to be fit to just lower than an amplitude value, but the more close to this value, the better.

Considering the assembly problems between ultrasonic horn and outside in the practical work, the flange with the thickness of 3 mm and the external diameter of 61 mm was added onto the displacement node (nodal section) of the ultrasonic horn. The modal analysis chart of the ultrasonic horn adding flange structure is shown in Figure 5. From the figure it is evident that resonance frequency of the ultrasonic horn is 20.075 kHz at the moment; that is to say, resonance frequency of the ultrasonic horn almost remains invariant with and without the flange, which conforms to design requirements.

In addition, the clamping method used for securing the insert to the ultrasonic horn is very important in order to obtain maximum amplitude of vibration at the tool tip. Therefore, the installing form of ultrasonic horn and tool holder should be also considered in the application of UAT. As the connection of the ultrasonic horn and cutting tool requires simple mechanism, superior reliability, cutting tool to be changed conveniently, and ultrasonic energy to be

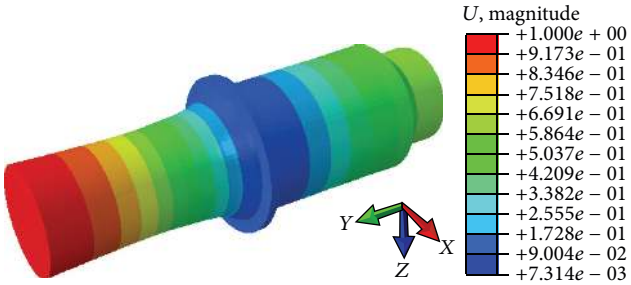

Modal analysis of ultrasonic horn
ODB: flange.odb Abaqus/standard 6.14-1 Wed Jul 22, 09:48:06
Central daylight time 2015
Step: modal analysis
Mode 10: value = 1.59096E + 10 freq. = 20075 (cycles/time)
Primary var.: U, magnitude
Deformed var.: U deformation scale factor: +1.390e + 01

Figure 5: Modal analysis chart of horn with flange.

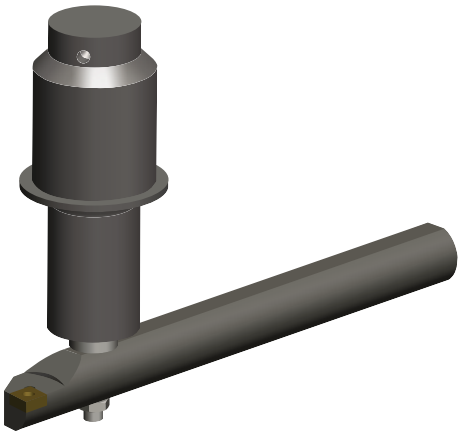

Figure 6: Ultrasonic horn clamped on tool holder.

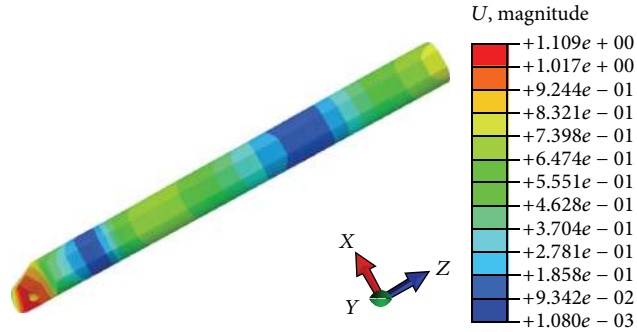

Modal analysis of tool holder
ODB: tool.odb Abaqus/standard 6.14-1 Tue Jul 28, 16:49:00
Central daylight time 2015
Step: modal analysis
Mode 10: value = 1.58466E + 10 freq. = 20035 (cycles/time)
Primary var.: U, magnitude
Deformed var.: U deformation scale factor: +2.780e + 01

Figure 7: Modal analysis graphic of tool holder with cutting tool.

transmitted efficiently, the pontes do not give out heat or only give out little heat while working continuously and make no screams. In this study, thread connection method, where tapped hole and through hole were manufactured on the small end of the ultrasonic horn and the tool holder, respectively, and where a special screw was designed to enable the ultrasonic horn to fasten with the tool holder as a whole, was adopted. Figure 6 shows the connecting format of the ultrasonic horn and tool holder.

A cutting tool was also fixed to the tool holder by using a standard high tensile screw. Figure 7 shows the modal analysis graphic of tool holder with the cutting tool installed. It can be seen from the figure that the resonance frequency of the tool holder and the cutting tool is 20.035 kHz, which approximates to theoretical design requirements. And the tool holder, cutting tool, and the acoustic head have the same resonance frequency. There is large damping between the tool holder system and the carriage (cross slide) of the lathe machine in this case; thus, a lot of formant can be simultaneously restrained under the conditions of wide band random vibration and noise, which can make the vibration change into thermal energy to be sent out so as to attain damping vibration attenuation. Figure 8 shows the structure of tool mounting.

With regard to the integral installation of MS-UAT, the tool mounting and the cutting tool were installed first. Assuring the tool holder was installed vertically, if not, it would give rise to uneven stress, which would damage the cutting tool and then could not achieve the considerable effect. After the cutting tool was installed, the ultrasonic horn and the ultrasonic transducer were installed in turn to ensure clean contact surface, so as not to affect the wave propagation. The designed MS-UAT was longitudinal ultrasonic vibration system. And the high-frequency vibration direction was the main cutting force direction. Therefore, it should be assured that the central axis of the ultrasonic transducer and ultrasonic horn were vertical with the horizontal plane of tool mounting, namely, the horizontal plane of machine tool. The power supply should be turned off before the signal line of the ultrasonic generator and ultrasonic transducer was connected to avoid electric shock. After the ultrasonic generator ran smoothly, UAT was started on.

The whole experimental system of UAT was constituted by a machine tool, an ultrasonic generator, an ultrasonic transducer, an ultrasonic horn, a tool mounting, a cutting tool, and so forth. The ultrasonic vibration system, cutting tool, and process unit are shown in Figure 9. The designed MS-UAT met the following requirements: when the tool holder clamped on the ultrasonic horn, it became a resonance system with the whole vibration device; after the tool holder clamped on the ultrasonic horn, the vibrational frequency of the system kept constant. The system had advantages of low mechanical loss, large output amplitude, high power transmission efficiency, and so forth.

3. Experimental Work

3.1. Workpiece and Cutting Tool. UAT tests were performed in dry condition using lathe type CA6140 with ultrasonic

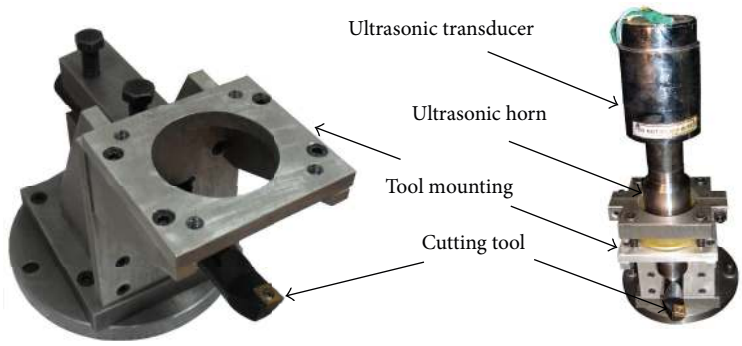

Figure 8: Fixture structure of ultrasonic vibration system.

Figure 9: Photograph of experimental setup.

vibration. The workpiece material used in this investigation was 0Cr18Ni9, 304 stainless steel which belongs to austenite structure. The chemical compositions of austenitic stainless steel are mainly Cr and Ni. It presented austenite structure after quenching, and its physical and mechanical properties had a significant effect on the character of its cutting process. The physical and mechanical properties of workpiece material are listed in Table 1. The machinability of ASS 304 was inferior [24, 25], especially when the cutting tool material, cutting edge geometry, and processing conditions were improper, or when the machine rigidity was poor, the difficult machinability of ASS 304 was more notable.

In the experiment, workpiece diameters were 33.5 mm, 35 mm, and 18 mm, respectively. Three different workpiece diameters were adopted to obtain different cutting speed. There were no direct relations between the surface roughness and the spindle speed of lathe through the analytical investigation, so the cutting speed was used to conduct experimental analysis in this study. Cutting speed Vc is an instantaneous speed of one point on the cutting edge of cutting tool relative to the waiting process surface on the main motion direction. It is described by the following relation:

$$Vc = \frac{\pi DN}{1000}, \tag{2}$$

where D is the workpiece diameter and N is the spindle speed of lathe. The transforming relationship of cutting speed and workpiece diameter calculated by the above formula is listed in Table 2.

Table 1: Physical and mechanical properties of workpiece material.

Properties	Value
Workpiece material	304 austenitic stainless steel
Workpiece diameter (mm)	33.5, 35, and 18
Elastic modulus (GPa), at room temperature	193
Density (kg/m^3)	8000
Poisson's ratio	0.3
Ultimate tensile strength (MPa)	515
Specific heat capacity (J/kg·K)	500
Thermal conductivity (W/m·K)	16.2
Coefficient of thermal expansion (m/°C)	17.8

In the machining process of ASS 304, the work hardening was severe, the cutting force was big, the cutting temperature was high, and the cutting tool wore out easily, so realizing high efficiency machining of ASS 304 should choose cutting tool material with good red hardness and abrasion resistance and should use suitable cutting tool angle and machining parameters. To the difficult-to-cut characteristic of ASS 304, CCMT120404-HM YBM251 type cemented carbide coated cutting tool with high hardness and preferable abrasion resistance was employed in this experiment to conduct UAT experiment. Geometric parameters of cutting tool had a significant effect on machining quality and cutting tool life. CCMT120404-HM YBM251 type cutting tool geometry is shown in Figure 10, and the mechanical specifications and features of cutting tool are listed in Table 3.

3.2. Experimental Analysis Method. Machined surface quality of workpiece had direct and significant effect on its usability (like fatigue strength, corrosion resistance, abrasion resistance, etc.) [26–28]. When two workpieces rubbed each other, the summits of surface were soon squashed flat and the severe wear came into being, thus affecting the match property of workpiece. At the same time, the corrosion resistance of rough surface was inferior in comparison with that of smooth surface, and this could be attributed to the corrosive substances easily gathered together in the

Table 2: Transforming relationship of cutting speed and workpiece diameter used in the experiment.

Cutting speed (m/min)	18	21	22	23	25	28	34	42	47
Workpiece diameter (mm)	18	33.5	35	18	18	18	33.5	33.5	33.5
Spindle speed of lathe (rev/min)	320	200	200	400	450	500	320	400	450

Table 3: Mechanical specifications and features of cutting tool.

Specifications and features	Value
Cutting tool material	Micrograin cemented carbide
Cutting tool part number	CCMT120404-HM YBM251
Cutting tool coating	TiC-Al_2O_3-TiN
Cutting edge length L (mm)	12.9
Inscribed circle diameter Φ I.C (mm)	12.7
Corner radius r (mm)	0.4
Nose angle (°)	80
Relief angle of main cutting edge (°)	7
Mounting-hole diameter Φd (mm)	5.56
Tool thickness S (mm)	4.76

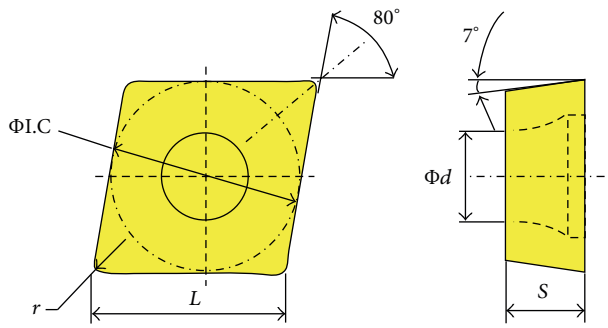

Figure 10: CCMT120404-HM YBM251 type cutting tool geometry.

valleys and cracks of the rough surface as well as gradually expanding its corrosive action. Additionally, under the action of external force, the rough surface was prone to produce stress concentration making microcracks be generated in the workpiece surface, and the fatigue strength of workpiece was subsequently reduced.

In view of the above information, the machined surface quality was mainly analysed in this paper, and the surface topography and surface roughness of machined workpiece were analysed to measure the machined surface quality. But due to the instability and boundedness of 2D evaluation parameters, 3D morphology evaluation parameters were used to evaluate the waviness and roughness and showed their advantages of the rich information and accurate evaluation [29]. Hence, 3D morphology evaluation parameters were adopted here to availably characterize the surface properties of machined workpiece.

The roughness parameters included arithmetic mean deviation, root mean square deviation, 10-point height, maximum height of summits, and maximum depth of valleys. The two main roughness parameters were the arithmetic mean deviation Sa and root mean square deviation Sq of 3D surface topography [30]. Therefore, the roughness parameters Sa and Sq were focused on in this study. It was exceedingly accurate that two parameters were adopted here.

The roughness parameter Sa is defined as the arithmetic mean of the absolute surface asperity departures from the reference plane within the sampling area [30]. It is contained within almost all the 3D surface profilers, so it is widely employed to evaluate surface roughness by numerous institutions. Sa can be expressed using the following equation [31, 32]:

$$Sa = \frac{1}{S}\iint_s l(x, y, z)\, dx\, dy = \frac{1}{MN}\sum_{j=1}^{N}\sum_{i=1}^{M}\left|\eta\left(x_i, y_j\right)\right|. \quad (3)$$

The roughness parameter Sq is defined as the root mean square value of asperity departures of a surface from the reference plane within the sampling area, which is equivalent to the standard deviation σ in statistics, so it is an ideal evaluation parameter [29, 30]. Sq can be calculated using the following equation [31, 32]:

$$\begin{aligned} Sq &= \sqrt{\frac{1}{S}\iint_s l^2(x, y, z)\, dx\, dy} \\ &= \sqrt{\frac{1}{MN}\sum_{j=1}^{N}\sum_{i=1}^{M}\eta^2\left(x_i, y_j\right)}, \end{aligned} \quad (4)$$

where $l = l(x, y, z)$ is the offset distance from any sampling point (x, y, z) to reference plane, S is the orthogonal projection of sampling area on the reference plane, $\eta(x, y)$ is the distance between every sampling point (x, y, z) and reference plane, and M and N are the number of sampling points in the x and y direction, respectively.

3.3. Experimental Details. The process parameters of the study mainly included ultrasonic vibration parameter and cutting parameter. The ultrasonic vibration parameters contained ultrasonic amplitude and vibrational frequency, and the cutting parameters contain feed rate, depth of cut, and cutting speed. In this experiment, the vibrational frequency was fixed at 20 kHz. Four process parameters and their levels used in the experiment are listed in Table 4.

Based on the theory of machined surface geometric features, the influence rule and mechanism of ultrasonic vibration parameters and cutting parameters on machined surface quality were analytically investigated, through the contrast test of the surface topography and surface roughness in turning of ASS 304 with and without ultrasonic vibration.

Table 4: Process parameters and their levels used in the experiment.

Process parameters	Symbol	Unit	Level 1	Level 2	Level 3	Level 4	Level 5
Ultrasonic amplitude	A	μm	0	15	23	30	—
Feed rate	f	mm/rev	0.08	0.1	0.15	0.2	—
Depth of cut	ap	mm	0.05	0.1	0.15	0.2	—
Cutting speed	Vc	m/min	18	21	22	23	And so forth

The influence of ultrasonic amplitude, feed rate, depth of cut, and cutting speed on the machined surface quality was mainly analysed in this paper; thereby, the mutual relation among these process parameters was effectively controlled. The high-quality and high-efficient processing was ultimately achieved.

Figure 11: Differences of the machined surface between UAT and CT.

4. Results and Discussion

The surface topography and surface roughness are the significant indicators in the process of measuring the machined surface quality. In this experiment, the MiCROMEASUR2 type 3D surface profiler manufactured by France STIL Company, which can conduct noncontact measurement on the machined surface and have 40000 data scanned and sampled evenly in each measurement with the accuracy rate $\pm 0.01\,\mu$m, is adopted to measure the 3D surface topography and surface roughness of machined workpiece. A $0.2 \times 0.2\,\text{mm}^2$ scanning area is chosen on the machined surface to measure the 3D surface topography and surface roughness. All values of surface roughness obtained from UAT and CT are listed in Table 5.

4.1. Study of 3D Surface Topography of Machined Workpiece. The surface topography of machined workpiece is formed with the interaction of various influence factors in the machining process, which is the microtopography and geometric feature of the different traces left by the cutting tool on the workpiece surface. The surface topography, which directly relates to the machining precision of workpiece, is a significant character to evaluate the machined surface quality. The surface topography of machined workpiece not only has direct effects on operational performance of components, but also has great effects on working performance of the whole equipment.

Acting as a special machining method, UAT adopts the vibration of high frequency and low amplitude in the machining, which makes the cutting tool and workpiece produce impact effect in the cutting process. The loading rate of the workpiece is great, and the inertial effect of materials has to be taken into account. The chip removal which is under the effect of impacting on cutting force is researched by the fracture dynamics method. With regard to a certain spot before the tip of crack, which is cracked on the tool nose in the cutting areas, the stress wave velocity caused by the vibration of the cutting tool producing impact is greater than the velocity of cutting tool movement. When the chip removal effects are generated before the cutting tool moves onto the location, the inner stress of the spot has already reached up to the ultimate strength of the materials so as to make it crack on account of the role of dynamic stress intensity factor. Namely, the crack initiation occurred on the spot. Providing that there are forces constantly acting on the crack initiation area in the next time, crack growth could be realized only by relatively small force. Therefore, the cutting process is conducted along with very small cutting force when the insert arrives at this position. This is the material removal mechanism of machined surface in UAT.

As the material removal mechanism and the formation mechanism of machined surface in UAT are all different from those in CT, this results in the fact that the machined surface quality is exceedingly different from that in CT as well. The UAT is analysed in comparison with the CT by means of the experiment, and at the same time the surface properties of the workpiece of ASS 304 in turning under different ultrasonic amplitudes are experimentally analysed.

4.1.1. Analysis of 3D Surface Topography in UAT and CT. Under the same condition, the designed MS-UAT was employed to make turning experiment with and without ultrasonic vibration on the workpiece of ASS 304. Figure 11 shows the workpiece after turning, and different areas represent the machining effects of UAT and CT, respectively. From the figure it is evident that there are distinctions between the machined surface of UAT and that of CT. The workpiece surface obtained by UAT is dull but smooth, and the workpiece surface obtained by CT is bright.

The super depth-of-field 3D display system is applied to observe and photograph the workpiece surface, and then the surface topography in UAT and CT is obtained, which is magnified 200 times, as shown in Figure 12. The machined surface obtained by CT is shown in Figure 12(a) and the results show that the deeper tooth marks are distributed evenly in the surface, and there are many different shades of grooves among the tooth marks. Figure 12(b) shows that during UAT the grains of machined surface are complex. Besides the lengthways feed marks, they also alternates with numerous transverse stripes, which form rotavirus grids. On account of the supplementary role of ultrasonic vibration, the machined surface shows some oscillation marks which are similar to ripple. The phenomenon that the depth of the

Table 5: Surface roughness in UAT and CT used for experimental results.

Number	Process parameters				Surface roughness			
					UAT		CT ($A = 0$)	
	f (mm/rev)	ap (mm)	Vc (m/min)	A (μm)	Sa (μm)	Sq (μm)	Sa (μm)	Sq (μm)
1	0.08	0.1	22	15	1.72	2.17	1.83	2.24
2	0.08	0.1	22	23	1.44	1.80	1.83	2.24
3	0.08	0.1	22	30	1.61	2.01	1.83	2.24
4	0.08	0.1	21	23	1.34	1.66	1.56	1.88
5	0.1	0.1	21	23	1.54	1.96	1.65	2.02
6	0.15	0.1	21	23	1.69	2.11	2.02	2.51
7	0.2	0.1	21	23	1.71	2.13	1.89	2.32
8	0.08	0.05	21	23	1.31	1.63	1.51	1.83
9	0.08	0.1	21	23	1.34	1.66	1.56	1.88
10	0.08	0.15	21	23	1.49	1.86	1.81	2.30
11	0.08	0.2	21	23	1.60	2.01	1.81	2.24
12	0.08	0.1	18	23	2.22	2.70	1.47	1.87
13	0.08	0.1	21	23	1.34	1.66	1.56	1.88
14	0.08	0.1	22	23	1.44	1.80	1.83	2.24
15	0.08	0.1	23	23	1.68	2.12	1.77	2.19
16	0.1	0.1	18	23	2.63	3.22	—	—
17	0.1	0.1	21	23	1.60	2.01	—	—
18	0.1	0.1	23	23	1.46	1.83	—	—
19	0.1	0.1	25	23	1.40	1.73	—	—
20	0.1	0.1	28	23	1.60	2.01	—	—
21	0.1	0.1	33	23	1.63	2.04	—	—
22	0.1	0.1	42	23	1.80	2.27	—	—
23	0.1	0.1	47	23	1.85	2.34	—	—
24	0.1	0.1	22	15	1.73	2.16	—	—
25	0.1	0.1	25	15	1.37	1.72	—	—
26	0.1	0.1	28	15	1.64	2.04	—	—
27	0.1	0.1	33	15	1.67	2.09	—	—
28	0.1	0.1	42	15	1.86	2.36	—	—
29	0.1	0.1	47	15	1.97	2.51	—	—

machined surface has irregularity is improved, but it still exists.

The surface topography of machined workpiece measured by 3D surface profiler is shown in Figure 13. According to the figure, it is observed obviously that the surface microtopography and 3D surface topography in UAT are extremely different from those in CT. As can be seen from Figures 13(a) and 13(c), the surface streaks after being machined by CT are exceedingly irregular. Besides tooth marks, the grooves formed by cutting tool on the machined surface are left. The depth of the grooves is different, and there are obvious distinctions among the grooves. As shown from Figures 13(b) and 13(d), as ultrasonic vibration is exerted in turning, the groove defect of machined surface is noticeably decreased. Although the grains of machined surface are extremely complex, the overall distribution is exceedingly uniform and the peaks and valleys are well-defined, which is different from CT with irregular surface. The cut marks of machined surface in UAT are shallower, and the overall surface looks smooth and symmetrical, and the appearance becomes convex and concave grid shaped. The reason for this phenomenon is that ultrasonic vibration is added on turning, and the cutting tool is in the state of ultrasonic vibration with a certain amplitude and frequency, which is different from the idle state in CT, so the contact form of cutting tool and workpiece is changed. The cutting tool and workpiece material are in the intermittent contact state in UAT. Hence, it takes a period of time for the workpiece material to recover when it goes through elastic deformation after suffering the shearing splitting. This can decline the degree of the material deformation, the heat generated by material deformation is decreased, and the cutting temperature is reduced, thus declining the phenomenon of surface burning and cracking in cutting process [33, 34].

The density distribution of the height of 3D surface topography can intuitively reflect the probability of the surface height and the overall distribution of machined surface in the height direction, and it has a significant impact on the lubrication and contact performance of the machined surface. Figures 14(a) and 14(b) are the surface height probability

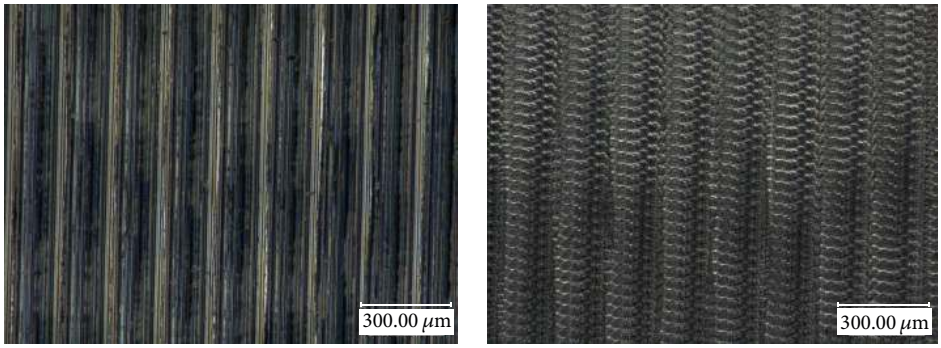

(a) CT (b) UAT

Figure 12: Surface topography magnified 200 times in UAT and CT.

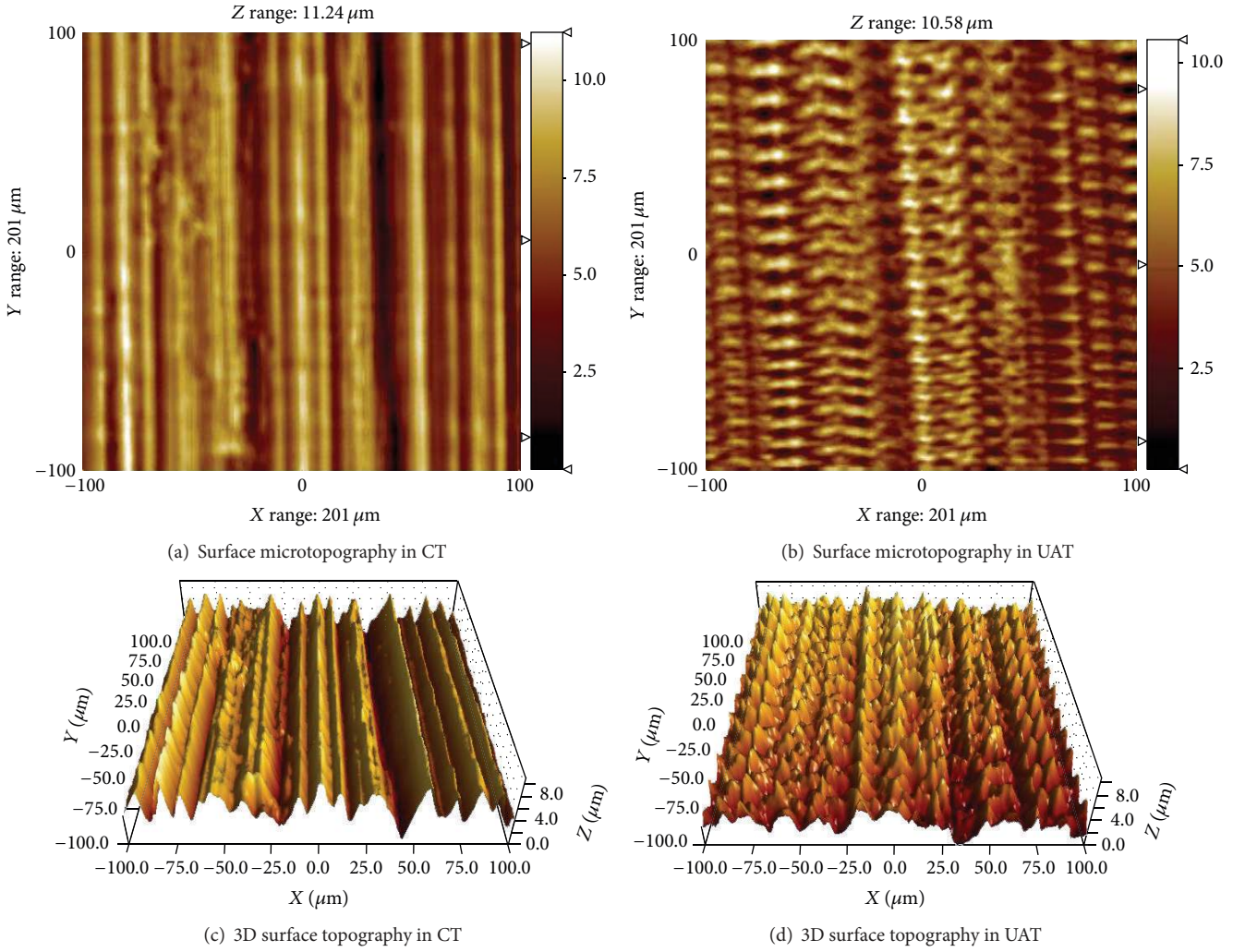

(a) Surface microtopography in CT

(b) Surface microtopography in UAT

(c) 3D surface topography in CT

(d) 3D surface topography in UAT

Figure 13: Surface microtopography and 3D surface topography in UAT and CT.

distribution histograms of the 3D surface topography of machined workpiece. The histogram shows the size of the proportion of peak and valley and surface roughness as well as abrasion resistance. Comparing the cutting effects in turning with and without ultrasonic vibration, it is evident from the figure that the probability of the height of 3D surface topography in 6~11.24 μm in CT is much greater than that in UAT, and it indicates that the surface roughness in CT is greater than that in UAT. It demonstrates that the machined surface quality of UAT is superior in comparison with that

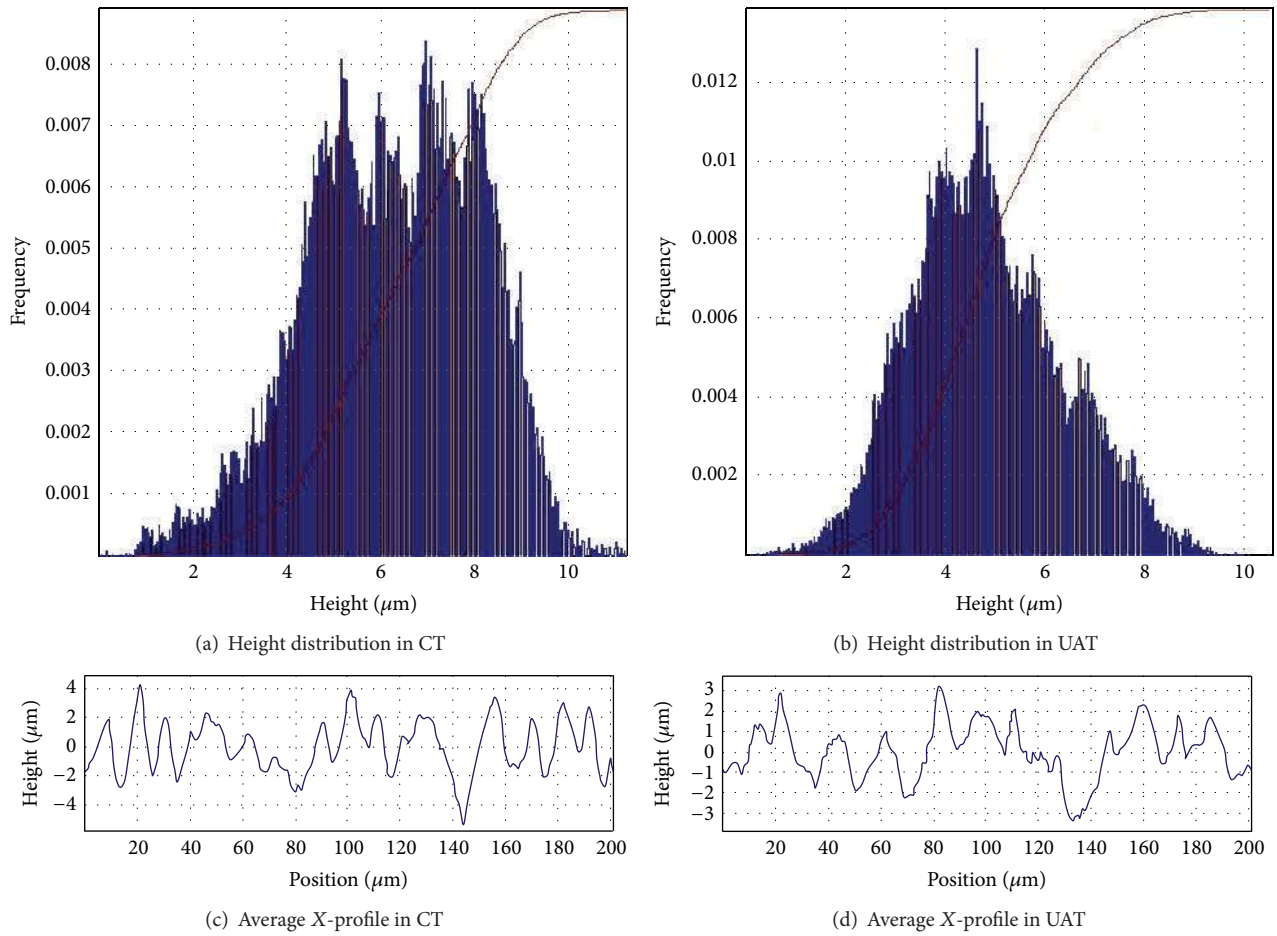

(a) Height distribution in CT

(b) Height distribution in UAT

(c) Average X-profile in CT

(d) Average X-profile in UAT

FIGURE 14: Height distribution histogram and average X-profile of the main image.

of CT. Additionally, Figures 14(c) and 14(d) are the average X-profile of the 3D surface topography image. As can also be seen from the figure, the maximum peak-to-valley height of 3D surface topography of machined workpiece in UAT is lower than that in CT.

In the cutting process, although the cutting edge of the cutting tool is ground sharply and the surface of the cutting tool is extremely smooth as well, the cutting tool leaves clear scratches on the workpiece after scratching because the cutting tool has corner radius and it is in motion. The formation mechanism of machined surface in CT is simple, it is mainly that a series of parallel tooth marks is left by the cutting tool when scratched on the workpiece surface, the cutting tool and workpiece are in the contact status all the time, and the chip flied off from the rake face so that it cannot be sheared. The chips are continuous filament and are wrapped on the workpiece surface with workpiece rotating, thus leaving some scratches on the workpiece surface. When UAT is adopted, no series of simple tooth marks are left on the machined surface at all, but the left scratches, which are left by cutting tool after cutting chips off. This can be explained by the fact that the cutting tool alters the cutting direction at any moment and the reciprocating cutting process takes place during each vibration cutting cycle, and each successive chip may be cut off by the operating cutting tool when UAT is exerted. Additionally, due to the cutting tool and workpiece in a state of intermittent contact, the material has a temporary relief process in the process of the shearing splitting. Before the microcrack produced in the cutting process continues to extend, it has already been cut off by the cutting tool of the next cutting process. Therefore, the size of the scallops left in the surface can be decreased.

4.1.2. Analysis of 3D Surface Topography under Different Ultrasonic Amplitudes. In order to study the influence of ultrasonic vibration on the machining effect of ASS 304, this paper compares the distinction of turning under different ultrasonic amplitudes by changing the ultrasonic amplitude (resp., 0 μm, 15 μm, 23 μm, and 30 μm) to study the influence of the ultrasonic amplitude on the 3D surface topography in the same processing conditions and environment. The comparative results are shown in Figures 15 and 16.

As can be seen from Figures 15(a) and 16(a), when ultrasonic amplitude is 0 (that is to say ultrasonic vibration is not exerted), it is equal to CT at this moment, the cut marks of the workpiece surface are deep, the space between cut marks is wide, and the surface is bumpy and fairly rough.

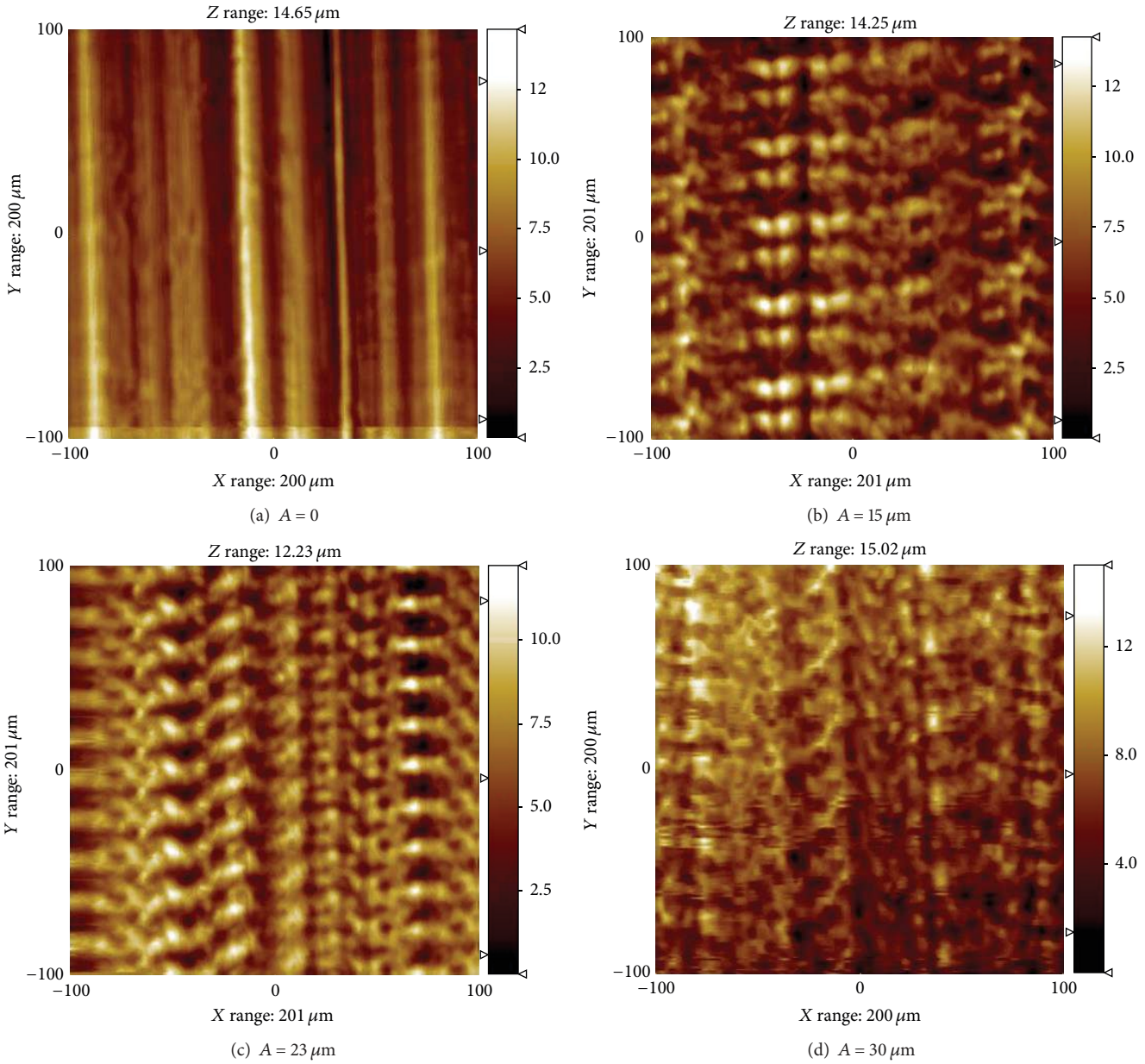

Figure 15: Surface microtopography of machined workpiece under different ultrasonic amplitudes.

From Figures 15(b) and 16(b), when ultrasonic amplitude is 15 μm, the cut marks of the workpiece surface are relatively uniform compared to CT as a whole, but parts of those show bulge, markings, and small hole, and this can be attributed to the defect of the workpiece itself. From Figures 15(c) and 16(c), when ultrasonic amplitude is 23 μm, the size of the cut marks of the workpiece surface is uniform, the cut marks are shallow, and the space between two cut marks is small, the marks look delicate and uniform, and the surface is symmetric and smooth. From Figures 15(d) and 16(d), it is observed that when ultrasonic amplitude is 30 μm, the textures of the workpiece surface and the size of cut marks are nonuniform, the cut marks are extremely deep, the space between two cut marks is wide, and it is significantly noticeable that the machined surface is rugged. The surface looks exceedingly indistinct and rough.

Based on fractal geometry theory, the root mean square wavelength $S_{\lambda q}$ of 3D surface, in the α direction, obtained by (4), is shown as follows [35]:

$$S_{\lambda q}(\alpha) = 2\pi \frac{S_q}{S_{\Delta q}(\alpha)} = 2\pi \sqrt{\frac{m_{00}}{m_{20}\cos^2\alpha + 2m_{11}\cos\alpha\sin\alpha + m_{02}\sin^2(\alpha)}}, \quad (5)$$

where $S_{\Delta q}$ is the root mean square slope value of the 3D surface within the sampling area, at angle α to the X positive

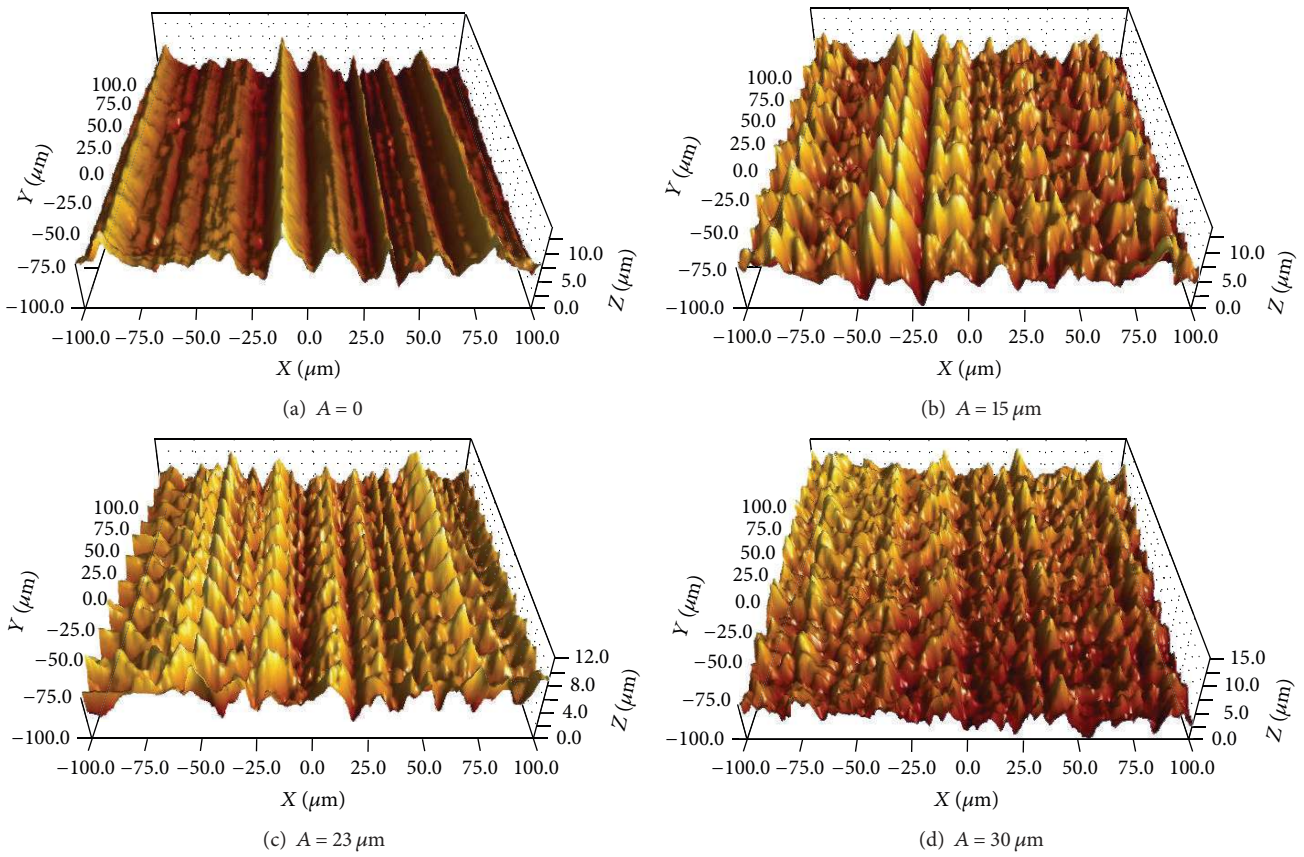

FIGURE 16: 3D surface topography of machined workpiece under different ultrasonic amplitudes.

direction; m_{00} is the zero-order surface spectral moment, denoting the height variances of the surface; m_{20} and m_{02}, which are the second surface spectral moments, denote the variances of slope in two vertical directions (X and Y measurement axes); m_{11} is the association variance of slope in these two directions. It is more reasonable to evaluate the root mean square wavelength of 3D random surface in the principal direction; that is,

$$S_{\lambda q} = S_{\lambda q}\left(\theta_p\right) = 2\pi\sqrt{\frac{2m_{00}}{m_{20}+m_{02}+\left[\left(m_{20}-m_{02}\right)^2+4m_{11}^2\right]^{1/2}}}, \quad (6)$$

where θ_p is the angle between the line of the principal direction and the X-axis. Supposing the surface wave is a sinusoid wave, of which the amplitude is A and frequency is ω, thus the root mean square wavelength $S_{\lambda q}$ can be obtained by the above equations [35]:

$$S_{\lambda q} = \frac{2\pi}{\omega}. \quad (7)$$

It can be seen from the equation above that the amplitude has no effects on root mean square wavelength. If the motion of insert is purely in principal direction, the amplitude does not affect the topography. However, Figure 16(a) is equal to CT, and Figures 16(b), 16(c), and 16(d) belong to UAT. Because of the subsidiarity of ultrasonic vibration, turned surface would show some vibration marks similar to the ripples. Consequently, 3D surface topography in UAT and that in CT are different. Additionally, with regard to 3D surface topography in UAT, they are the same on the whole. But the height of the surface vibration marks is somewhat different on account of the amplitude.

In general, when ultrasonic amplitude is 23 μm, the cutting effect is superior in comparison with that under other ultrasonic amplitudes, the values of surface roughness obtained from the experimental data are smaller, but there is a certain surface defect because of the influence of other factors. The machined surface quality can be promoted by optimizing cutting parameters (such as feed rate, depth of cut, and cutting speed).

4.2. Influence of Process Parameters on Surface Roughness of Machined Workpiece. The surface roughness of machined workpiece, which has great influence on the usability of components, reflects the irregular microcosmic height of the machined surface. Provided that surface roughness is oversize, it can reduce the strength, abrasion resistance, and corrosion resistance of components and also has a great influence on the appearance of components and the accuracy of measurement. The size of surface roughness

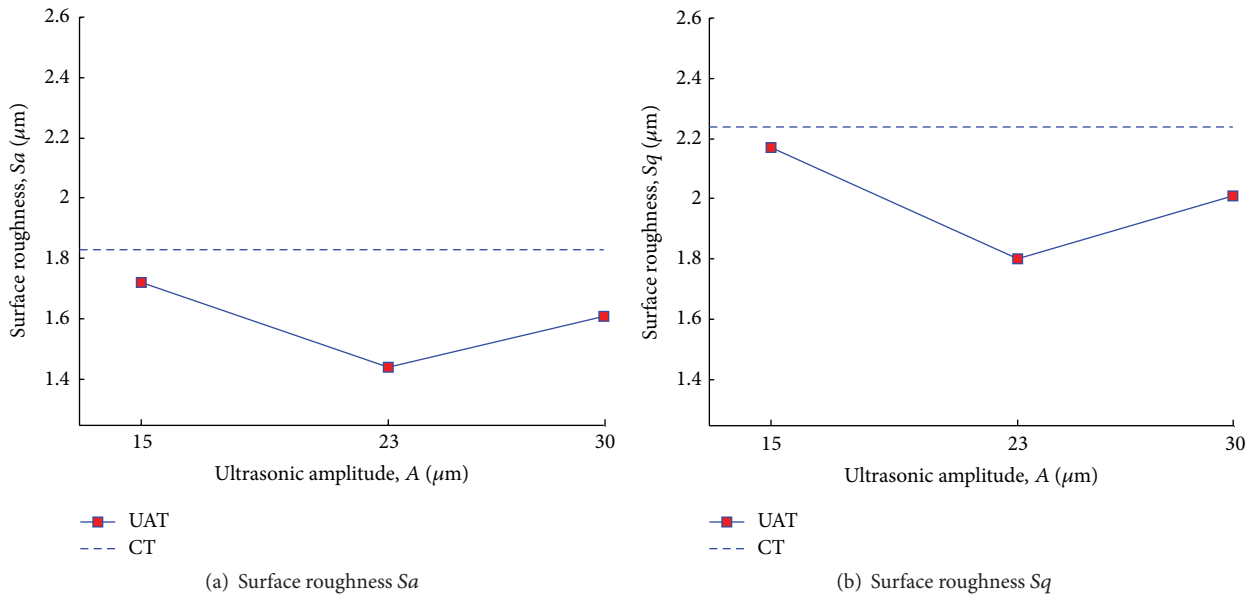

(a) Surface roughness *Sa*

(b) Surface roughness *Sq*

Figure 17: Relation curve of surface roughness changed with ultrasonic amplitude.

directly impacts the entire working performance and lifetime of components. In UAT, the principal factors affecting the surface roughness are ultrasonic amplitude, feed rate, depth of cut, cutting speed, and so forth. The influence rule of the ultrasonic amplitude, feed rate, depth of cut, and cutting speed and other principal factors on the surface roughness of the workpiece of ASS 304 is experimentally analysed to get an optimized combination of the process parameters.

4.2.1. Influence of Ultrasonic Amplitude on Surface Roughness. The influence of the ultrasonic amplitude A on the surface roughness of machined workpiece in UAT of ASS 304 is studied. The following cutting conditions are used in these experiments: $f = 0.08$ mm/rev, $ap = 0.1$ mm, $Vc = 22$ m/min, and $A = 15\sim30$ μm or $A = 0$ (CT). The relation curve of surface roughness changed with ultrasonic amplitude is shown in Figure 17. From the graph, it is observed that the whole variation trends of the surface roughness *Sa* and surface roughness *Sq* are basically the same. The surface roughness *Sa* and surface roughness *Sq* in UAT show a decreased tendency with increasing ultrasonic amplitude from 15 μm to 30 μm, but not to the extent that the smaller the ultrasonic amplitude is, the greater the surface roughness is. When the ultrasonic amplitude is 23 μm, the surface roughness is smaller, and this can be explained by the fact that continuous chip acquired at this moment results in the slight damage of the interface and the less surface defect [11, 14, 18].

From the point of ultrasonic vibration kinematics, although the vibration cutting can reach its full effects and the surface roughness has a larger downtrend when the ultrasonic amplitude is increased, the wear of cutting tool is decreased and the ironing effect of the flank face is weakened when the ultrasonic amplitude is increased [3, 11, 14, 18]. Hence, the downtrend of the surface roughness is not noticeable with increasing ultrasonic amplitude, which can only play a role in improving the critical cutting speed and the machining efficiency. Compared to CT, when the range of ultrasonic amplitude is 15~30 μm, the surface roughness *Sa* and surface roughness *Sq* in UAT are lower than those in CT. Therefore, exerting ultrasonic vibration and choosing appropriate ultrasonic amplitude (such as $A = 23$ μm) can contribute to improving machined surface quality.

4.2.2. Influence of Feed Rate on Surface Roughness. The influence of the feed rate f on the surface roughness of machined workpiece in turning of ASS 304 with and without ultrasonic vibration is also analytically studied. The following cutting conditions are used in this series of experiments: $f = 0.08\sim0.2$ mm/rev, $ap = 0.1$ mm, $Vc = 21$ m/min, and $A = 23$ μm or $A = 0$ (CT). Figure 18 shows the relation curve of surface roughness changed with feed rate. As shown from the graph, the whole variation trend of the surface roughness *Sa* is basically the same as that of the surface roughness *Sq*. The surface roughness *Sa* and surface roughness *Sq* in UAT increase with increasing feed rate from 0.08 to 0.2 mm/rev, whereas, with an increase in the feed rate from 0.15 to 0.2 mm/rev, the surface roughness almost does not change. Comparing CT and UAT, when feed rate is increased from 0.08 to 0.2 mm/rev, the surface roughness *Sa* and surface roughness *Sq* in UAT are lower than those in CT.

During machining, after the feed rate is increased, the width of the chip cutoff by each knife is increased, and the increase of chip area makes great obstacle for its discharge. That can result in making a mass of chip pile-up between the tool tip and machined surface. In this case, cutting system is more prone to tremors, and severe surface defect is caused after cutting. And wider chip, which convolves on the machined surface so that serious scratch of the cutting tool and machined surface is caused, is not easy to fracture. The damage of cutting tool can damage the surface quality

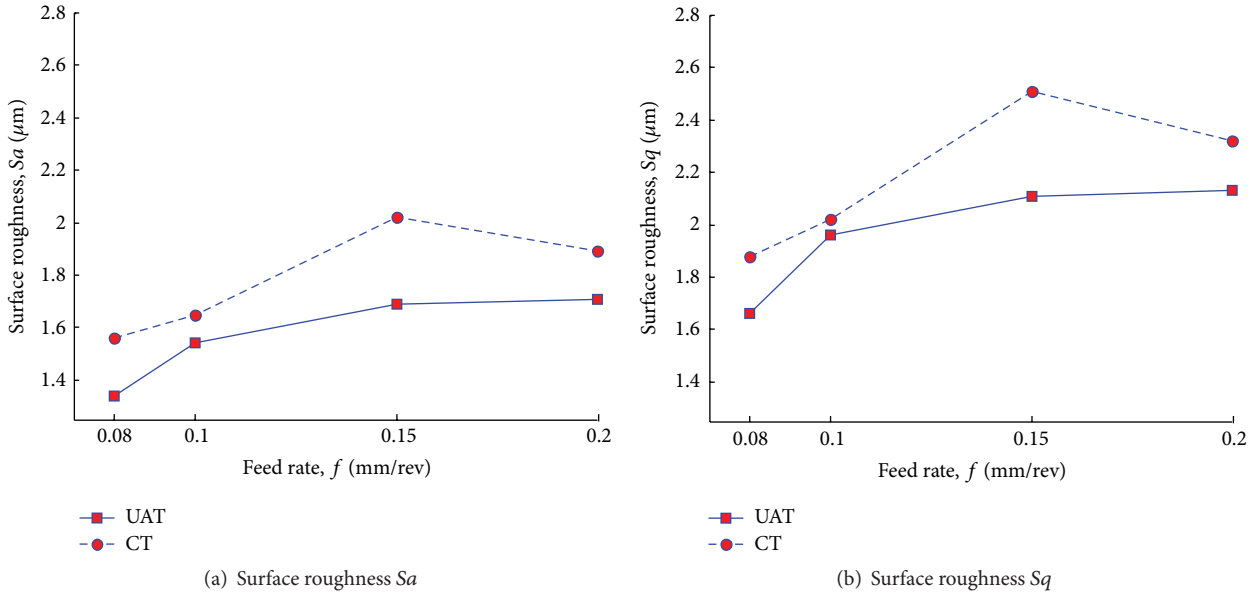

(a) Surface roughness *Sa* (b) Surface roughness *Sq*

FIGURE 18: Relation curve of surface roughness changed with feed rate.

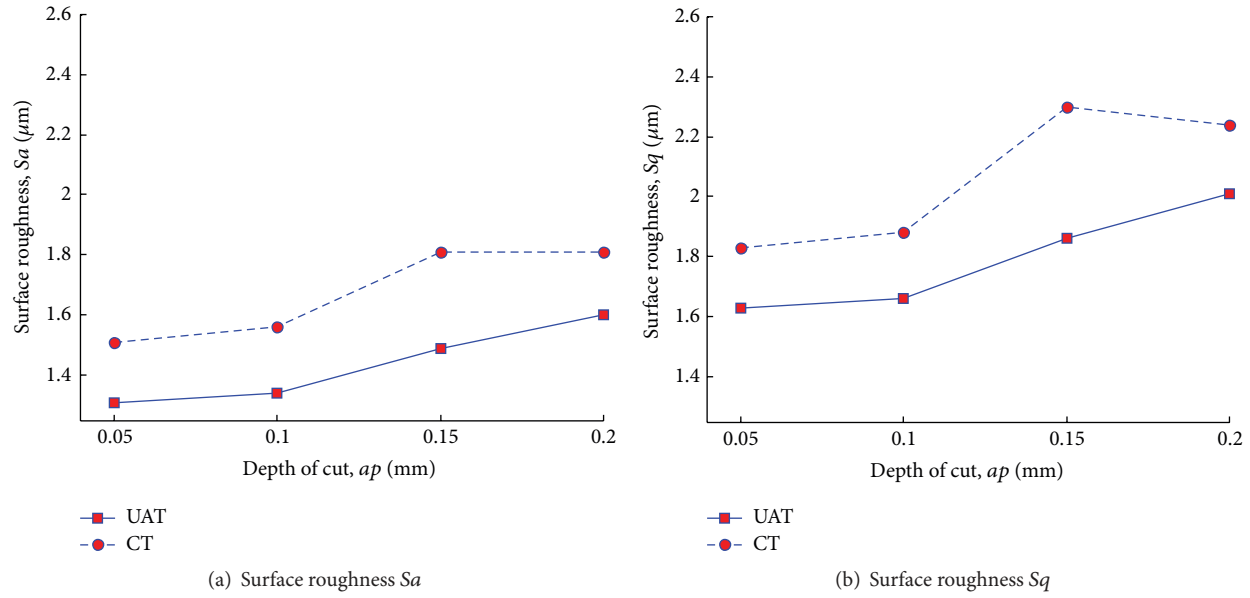

(a) Surface roughness *Sa* (b) Surface roughness *Sq*

FIGURE 19: Relation curve of surface roughness changed with depth of cut.

further. So in the real machining, choosing smaller feed rate (such as $f = 0.08$ mm/rev) can ensure the machined surface quality.

4.2.3. Influence of Depth of Cut on Surface Roughness. The influence of the depth of cut ap on the surface roughness of machined workpiece in turning of ASS 304 with and without ultrasonic vibration is also experimentally studied. The following cutting conditions are used in these tests: $f = 0.08$ mm/rev, $ap = 0.05$~0.2 mm, $Vc = 21$ m/min, and $A = 23\,\mu$m or $A = 0$ (CT). Figure 19 shows the relation curve of surface roughness changed with depth of cut. According to the graph, it can be seen that the whole variation trends of the surface roughness *Sa* and surface roughness *Sq* are basically the same. The surface roughness *Sa* and surface roughness *Sq* in UAT increase with increasing depth of cut from 0.05 to 0.2 mm, whereas when depth of cut is increased from 0.05 to 0.1 mm, the rangeability of surface roughness *Sa* and surface roughness *Sq* is not large. Compared to CT, the surface roughness *Sa* and surface roughness *Sq* in UAT are lower than those in CT as a whole.

The influence of depth of cut on machined surface quality mainly arises from the influence of it on cutting force. Increasing depth of cut makes cutting force increase.

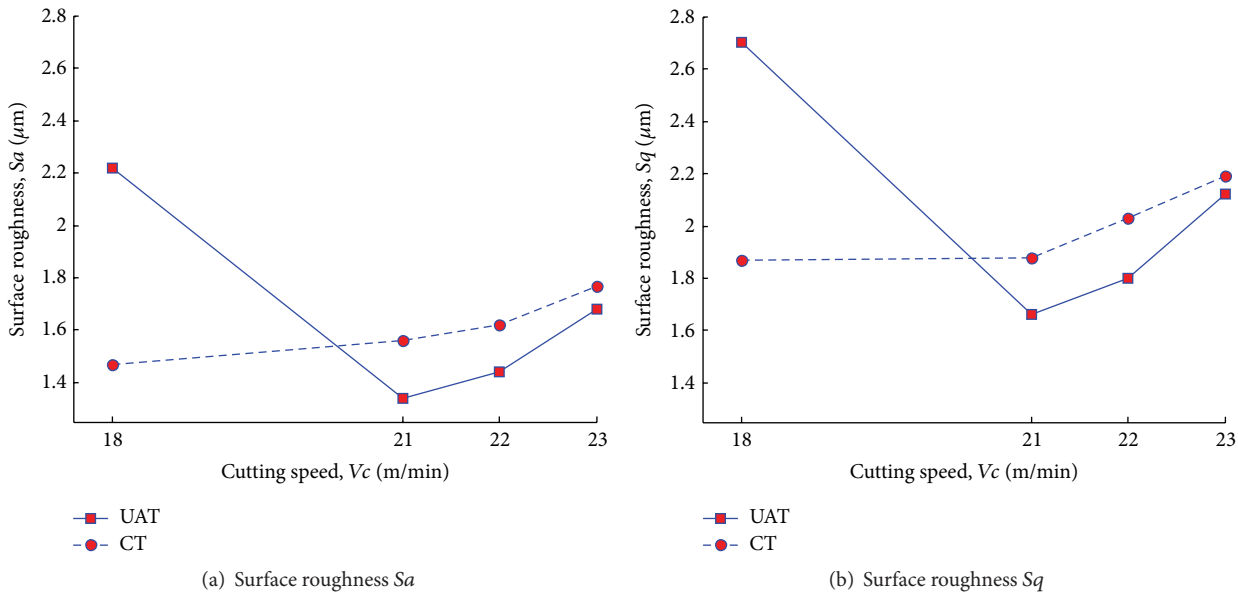

(a) Surface roughness *Sa*

(b) Surface roughness *Sq*

Figure 20: Relation curve of surface roughness changed with cutting speed.

This can make the extrusion of chip and rake face more serious and the reaction stronger, thus making the chip easily cement on the rake face of cutting tool to form built-up edge. Furthermore, larger depth of cut may give rise to machined surface deformed and bigger vibration, and so forth. With a growth in the depth of cut, the surface roughness of machined workpiece is increased. Hence, during machining, exerting ultrasonic vibration and choosing appropriate depth of cut (e.g., $ap = 0.1$ mm) can contribute to improving machining quality.

4.2.4. Influence of Cutting Speed on Surface Roughness. The influence of the cutting speed Vc on the surface roughness of machined workpiece in turning of ASS 304 with and without ultrasonic vibration is also experimentally analysed. The following cutting conditions are used in this series of tests: $f = 0.08$ mm/rev, $ap = 0.1$ mm, $Vc = 18$~23 m/min, and $A = 23\,\mu$m or $A = 0$ (CT). The relation curve of surface roughness changed with cutting speed is shown in Figure 20 and the results show that the whole variation trend of the surface roughness Sa is basically the same as that of the surface roughness Sq. Figure 20 further demonstrates that the general trend of the surface roughness Sa and surface roughness Sq in UAT is decreased first and then increased with increasing cutting speed from 18 to 23 m/min. Figure 20 also illustrates that the best surface roughness Sa and surface roughness Sq in UAT are obtained using a cutting speed of 21 m/min. And when the range of cutting speed is 20~23 m/min, the surface roughness Sa and surface roughness Sq in UAT are low in comparison with those in CT.

When cutting speed is lower, the surface roughness is bigger. This can be attributed to the fact that the action time of cutting tool on unit area is extended at low speed, and the increase of resilience value of machined surface makes friction heat increase, so the built-up edge and scale are prone to be produced, and the alternating stress frequently acts on machined surface, which increases the friction between cutting tool and machined surface. When cutting speed is accelerated, the material plastic goes down, the springback degree of machined surface is reduced, the effect of friction between flank face and machined surface is decreased, and the surface roughness is noticeably reduced. Nevertheless, after cutting speed is added up to 21 m/min, the condition for cutting heat to dissipate is inferior, so the cutting heat is accumulated on the machined surface, which enhances the friction and bond between the flank face and machined surface, and the surface roughness is gradually increased. When cutting speed is added up to a certain value, the effect of dissociation of cutting tool and workpiece produced by vibration is weakened, so the diffusion wear of cutting tool is aggravated; thereby the surface roughness is increased so that the process of UAT may verge on CT. In other words, in terms of the surface roughness of machined workpiece, UAT gets an optimum cutting speed range. The surface roughness in UAT is lower than that in CT during this range, and the best surface quality can be obtained.

In order to further study the influence of the cutting speed Vc on the surface roughness of machined workpiece in turning with ultrasonic vibration, the UAT tests of ASS 304 are conducted at the selected cutting conditions. The following two sets of cutting conditions are used in these tests: (i) $f = 0.1$ mm/rev, $ap = 0.1$ mm, $Vc = 18$~47 m/min, and $A = 23\,\mu$m; (ii) $f = 0.1$ mm/rev, $ap = 0.1$ mm, $Vc = 22$~47 m/min, and $A = 15\,\mu$m. Figure 21 shows the relation curve of surface roughness changed with cutting speed. According to the graph, it is observed that the whole variation trend of the surface roughness Sa and surface roughness Sq is basically the same. Compared to Figure 20, the variation trend of surface roughness in Figure 21 is decreased first and then increased with increasing cutting speed, which is the same as

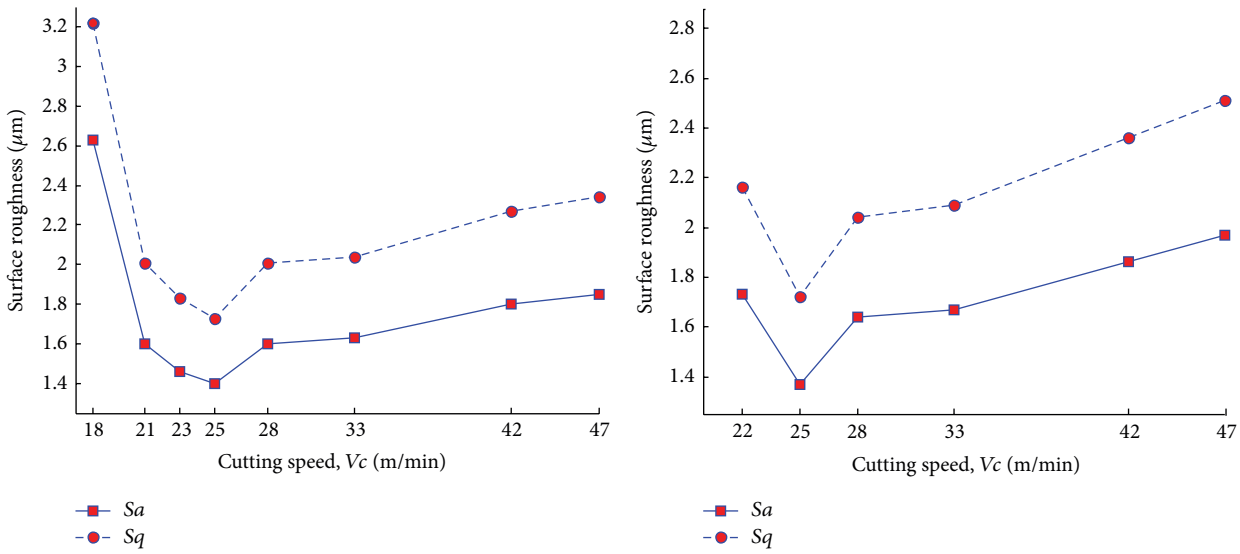

(a) f = 0.1 mm/rev, ap = 0.1 mm, and A = 23 μm

(b) f = 0.1 mm/rev, ap = 0.1 mm, and A = 15 μm

Figure 21: Relation curve of surface roughness changed with cutting speed.

that in Figure 20. But when surface roughness is the smallest, the value of cutting speed is changed. As can be seen from Figures 21(a) and 21(b), when the feed rate and the depth of cut keep constant, ultrasonic amplitude changed does not affect the value of cutting speed at the best surface roughness. As shown in Figure 20, when the feed rate is 0.08 mm/rev, the surface roughness is the smallest at a cutting speed of 21 m/min whereas, from Figure 21, when the feed rate is 0.1 mm/rev, the surface roughness is the smallest at a cutting speed of 25 m/min.

The surface roughness in UAT can be reduced distinctly by selecting appropriate process parameters. Firstly, due to high-frequency vibration of cutting tool, a huge accelerated speed is produced on the cutting direction, and sky-high kinetic energy is gathered on the tool tip, and then the workpiece material is instantly removed. But only a small amount of material on the shear band generates plastic deformation. Before the cracks caused by cracked materials on the shear band expand all around, the cutting tool has unloaded the force on the workpiece, thus reducing the chances of the surface tear. But materials, which have time to generate elastic deformation, get recovered modestly after the cutting tool leaves workpiece. So the plastic tearing and deformation of machined surface in UAT are all smaller than those in CT. Secondly, the cutting tool has a certain ironing effect on machined surface while reciprocating to slide on the workpiece surface. At higher temperatures, the mottling, microtear, fold, bulge, and microcrack on the surface are decreased on a certain level or even removed through the ironing of cutting tool. Subsequently, the continuous contact between the cutting tool and the workpiece is bad for heat loss during the process of CT. A wealth of cutting heat gathers on the machined surface, which can severely burn it. But UAT changes the primary static contact between the cutting tool and the workpiece, and cutting turns into interrupted cutting. Therefore, UAT can improve the surface roughness of machined workpiece.

5. Conclusions

In this study, a detailed experimental investigation is presented for the influences of ultrasonic amplitude, feed rate, depth of cut, and cutting speed on the machined surface quality in UAT of ASS 304 with cemented carbide coated cutting tool. The following conclusions are drawn from these experimental results.

(1) The comparison of UAT and CT of ASS 304: there were noticeable differences of the surface topography of machined workpiece. With CT, the surface streaks were quite irregular, and various shades of grooves scratched by cutting tool in the workpiece surface were left. And there were noticeable distinctions among grooves. The grains of the surface in UAT were complicated. The overall distribution of the grains was well distributed, and the appearance became convex and concave grid shaped. And the surface was extremely delicate compared to that of CT, but the brightness of the machined surface was inferior.

(2) When ultrasonic amplitude was 23 μm, the surface topography in UAT of ASS 304 was much better than other ultrasonic amplitudes and the CT. The size of cut marks of workpiece surface was well distributed, the cut marks were shallower, and the space between two cut marks was smaller; then it looked like more delicate and the surface was considerablely symmetric and smoother relatively. The surface roughness obtained from the experimental data was also smaller. But there was a certain surface defect on account of the influence of other factors. The machined surface

quality could be promoted by optimizing cutting parameters.

(3) In UAT of ASS 304, it was obvious that process parameters had effect on the surface roughness of machined workpiece. Under certain conditions, the smaller the ultrasonic amplitude was, the bigger the surface roughness was, and the surface roughness was decreased first and then increased with a growth in the ultrasonic amplitude. The surface roughness was increased with increasing feed rate and depth of cut, whereas, with an increase in the feed rate from 0.15 to 0.2 mm/rev, the surface roughness approximately kept constant. The surface roughness had no direct relation to the spindle speed of lathe, but cutting speed had great effect on it. The general trend of the surface roughness was decreased first and then increased with increasing cutting speed.

(4) There was an optimum cutting speed to enable the surface roughness to be minimum in UAT of ASS 304. The optimum cutting speed was inconstant, and it changed as feed rate and depth of cut changed and was irrelevant to ultrasonic amplitude. The surface roughness was the best at a cutting speed of 21 m/min under the cutting conditions of $f = 0.08$ mm/rev, $ap = 0.1$ mm, and $A = 23\,\mu$m, whereas when $f = 0.1$ mm/rev, $ap = 0.1$ mm, and $A = 15\,\mu$m or $A = 23\,\mu$m, the best surface roughness was obtained at a cutting speed of 25 m/min.

(5) It was visible that the surface roughness in UAT was superior compared to that in CT when appropriate process parameters were chosen in turning of ASS 304. The surface roughness in UAT was more preferable than that in CT using the following cutting conditions: (i) $f = 0.08$ mm/rev, $ap = 0.1$ mm, $Vc = 22$ m/min, and $A = 15$~$23\,\mu$m; (ii) $f = 0.08$~0.2 mm/rev, $ap = 0.1$ mm, $Vc = 21$ m/min, and $A = 23\,\mu$m; (iii) $f = 0.08$ mm/rev, $ap = 0.05$~0.2 mm, $Vc = 21$ m/min, and $A = 23\,\mu$m; (iv) $f = 0.08$ mm/rev, $ap = 0.1$ mm, $Vc = 20$~23 m/min, and $A = 23\,\mu$m.

(6) When process parameters were chosen reasonably in UAT of ASS 304, the surface roughness could be reduced prominently, and the surface topography also was promoted. The preferable surface topography and surface roughness could be obtained using the cutting conditions of $A = 23\,\mu$m, $f = 0.08$ mm/rev, $ap = 0.05$ mm or $ap = 0.1$ mm, and $Vc = 21$ m/min, and the machined surface quality of workpiece could satisfy the functional requirements of its usability in the engineering application.

Conflict of Interests

The authors declare that there is no conflict of interests regarding the publication of this paper.

References

[1] S. J. Zhang, S. To, S. J. Wang, and Z. W. Zhu, "A review of surface roughness generation in ultra-precision machining," *International Journal of Machine Tools and Manufacture*, vol. 91, pp. 76–95, 2015.

[2] K. Vivekananda, G. N. Arka, and S. K. Sahoo, "Finite element analysis and process parameters optimization of ultrasonic vibration assisted turning (UVT)," *Procedia Materials Science*, vol. 6, pp. 1906–1914, 2014.

[3] V. K. Astashev and V. I. Babitsky, *Ultrasonic Processes and Machines: Dynamics, Control and Applications*, Springer, Berlin, Germany, 2007.

[4] V. Babitsky and V. Astashev, "Nonlinear dynamics and control of ultrasonically assisted machining," *Journal of Vibration and Control*, vol. 13, no. 5, pp. 441–460, 2007.

[5] N. Ahmed, A. V. Mitrofanov, V. I. Babitsky, and V. V. Silberschmidt, "Analysis of forces in ultrasonically assisted turning," *Journal of Sound and Vibration*, vol. 308, no. 3-5, pp. 845–854, 2007.

[6] V. Ostasevicius, R. Gaidys, J. Rimkeviciene, and R. Dauksevicius, "An approach based on tool mode control for surface roughness reduction in high-frequency vibration cutting," *Journal of Sound and Vibration*, vol. 329, no. 23, pp. 4866–4879, 2010.

[7] V. P. Astakhov, *Modern Machining Technology A Practical Guide: Turning,*, Woodhead Publishing Limited, Cambridge, UK, 2011.

[8] L. Abhang and M. Hameedullah, "Parametric investigation of turning process on en-31 steel," *Procedia Materials Science*, vol. 6, pp. 1516–1523, 2014.

[9] T. B. Thoe, D. K. Aspinwall, and M. L. H. Wise, "Review on ultrasonic machining," *International Journal of Machine Tools and Manufacture*, vol. 38, no. 4, pp. 239–255, 1998.

[10] G. Ya, H. W. Qin, S. C. Yang, and Y. W. Xu, "Analysis of the rotary ultrasonic machining mechanism," *Journal of Materials Processing Technology*, vol. 129, no. 1–3, pp. 182–185, 2002.

[11] A. Maurotto, R. Muhammad, A. Roy, and V. V. Silberschmidt, "Enhanced ultrasonically assisted turning of a β-titanium alloy," *Ultrasonics*, vol. 53, no. 7, pp. 1242–1250, 2013.

[12] R. Muhammad, M. S. Hussain, A. Maurotto, C. Siemers, A. Roy, and V. V. Silberschmidt, "Analysis of a free machining α+β titanium alloy using conventional and ultrasonically assisted turning," *Journal of Materials Processing Technology*, vol. 214, no. 4, pp. 906–915, 2014.

[13] V. I. Babitsky, A. V. Mitrofanov, and V. V. Silberschmidt, "Ultrasonically assisted turning of aviation materials: simulations and experimental study," *Ultrasonics*, vol. 42, no. 1–9, pp. 81–86, 2004.

[14] S. Patil, S. Joshi, A. Tewari, and S. S. Joshi, "Modelling and simulation of effect of ultrasonic vibrations on machining of Ti6Al4V," *Ultrasonics*, vol. 54, no. 2, pp. 694–705, 2014.

[15] G. A. Volkov, V. A. Bratov, A. A. Gruzdkov, V. I. Babitsky, Y. V. Petrov, and V. V. Silberschmidt, "Energy-based analysis of ultrasonically assisted turning," *Shock and Vibration*, vol. 18, no. 1-2, pp. 333–341, 2011.

[16] M. Khajehzadeh, M. Akhlaghi, and M. R. Razfar, "Finite element simulation and experimental investigation of tool temperature during ultrasonically assisted turning of aerospace aluminum using multicoated carbide inserts," *International Journal of Advanced Manufacturing Technology*, vol. 75, no. 5-8, pp. 1163–1175, 2014.

[17] V. I. Babitsky, A. N. Kalashnikov, A. Meadows, and A. A. H. P. Wijesundara, "Ultrasonically assisted turning of aviation

materials," *Journal of Materials Processing Technology*, vol. 132, no. 1–3, pp. 157–167, 2003.

[18] C. Nath and M. Rahman, "Effect of machining parameters in ultrasonic vibration cutting," *International Journal of Machine Tools & Manufacture*, vol. 48, no. 9, pp. 965–974, 2008.

[19] K. Vivekananda, G. N. Arka, and S. K. Sahoo, "Design and analysis of ultrasonic vibratory tool (UVT) using FEM, and experimental study on ultrasonic vibration-assisted turning (UAT)," *Procedia Engineering*, vol. 97, pp. 1178–1186, 2014.

[20] K.-L. Kuo, "Ultrasonic vibrating system design and tool analysis," *Transactions of Nonferrous Metals Society of China*, vol. 19, supplement 1, pp. s225–s231, 2009.

[21] Q. Feng, C. Z. Ren, and Z. J. Pei, *Machining Technology for Composite Materials Principles and Practice: Ultrasonic Vibration-Assisted (UV-A) Machining of Composites*, Wood-Head Publishing Limited, Cambridge, UK, 2012.

[22] N. Ahmed, A. V. Mitrofanov, V. I. Babitsky, and V. V. Silberschmidt, "Analysis of material response to ultrasonic vibration loading in turning Inconel 718," *Materials Science and Engineering: A*, vol. 424, no. 1-2, pp. 318–325, 2006.

[23] Y. S. Xu, P. Zou, X. L. Yang, and Y. He, "Study on ultrasonic generator for ultrasonically assisted machining," *Advanced Materials Research*, vol. 797, pp. 320–325, 2013.

[24] M. A. Xavior and M. Adithan, "Determining the influence of cutting fluids on tool wear and surface roughness during turning of AISI 304 austenitic stainless steel," *Journal of Materials Processing Technology*, vol. 209, no. 2, pp. 900–909, 2009.

[25] M. Nalbant and Y. Yildiz, "Effect of cryogenic cooling in milling process of AISI 304 stainless steel," *Transactions of Nonferrous Metals Society of China*, vol. 21, no. 1, pp. 72–79, 2011.

[26] V. I. Babitsky, A. N. Kalashnikov, and F. V. Molodtsov, "Autoresonant control of ultrasonically assisted cutting," *Mechatronics*, vol. 14, no. 1, pp. 91–114, 2004.

[27] M. B. G. Jun, S. S. Joshi, R. E. DeVor, and S. G. Kapoor, "An experimental evaluation of an atomization-based cutting fluid application system for micromachining," *Journal of Manufacturing Science and Engineering*, vol. 130, no. 3, pp. 181–188, 2008.

[28] H. Aouici, M. A. Yallese, A. Belbah, M. F. Ameur, and M. Elbah, "Experimental investigation of cutting parameters influence on surface roughness and cutting forces in hard turning of X38CrMoV5-1 with CBN tool," *Sadhana*, vol. 38, no. 3, pp. 429–445, 2013.

[29] X. Cao, B. Lin, Y. Wang, and S. Wang, "Influence of diamond wheel grinding process on surface micro-topography and properties of SiO_2/SiO_2 composite," *Applied Surface Science*, vol. 292, pp. 181–189, 2014.

[30] R. A. Waikar and Y. B. Guo, "A comprehensive characterization of 3D surface topography induced by hard turning versus grinding," *Journal of Materials Processing Technology*, vol. 197, no. 1–3, pp. 189–199, 2008.

[31] R. K. Kumar, S. Seetharamu, and M. Kamaraj, "Quantitative evaluation of 3D surface roughness parameters during cavitation exposure of 16Cr-5Ni hydro turbine steel," *Wear*, vol. 320, no. 1, pp. 16–24, 2014.

[32] M. Arvinth Davinci, N. L. Parthasarathi, U. Borah, and S. K. Albert, "Effect of the tracing speed and span on roughness parameters determined by stylus type equipment," *Measurement*, vol. 48, no. 1, pp. 368–377, 2014.

[33] L. Yang, *Study of ultrasonic vibration precision cutting for plastic material [Ph.D. thesis]*, School of Mechatronics Engineering, Faculty of Mechanical Manufacturing and Automation, Harbin Institute of Technology, 2007.

[34] Z. M. Zhou, *Research on the stainless steel precise turned by natural diamond tool [Ph.D. thesis]*, School of Mechanical Engineering, Faculty of Mechatronic Engineering, Dalian University of Technology, 2010.

[35] C.-G. Li, S. Dong, and G.-X. Zhang, "Evaluation of the root-mean-square wavelength of machined 3D surface topography," *Wear*, vol. 232, no. 1, pp. 76–83, 1999.